Struct Multidisc Optim
DOI 10.1007/s00158-010-0493-y

RESEARCH PAPER

Effect of approximation fidelity on vibration-based elastic constants identification

Christian Gogu · Raphael Haftka · Rodolphe Le Riche · Jerome Molimard

Received: 30 August 2009 / Revised: 6 January 2010 / Accepted: 4 February 2010

Abstract Some applications such as identification or Monte Carlo based uncertainty quantification often require simple analytical formulas that are fast to evaluate. Approximate closed-form solutions for the natural frequencies of free orthotropic plates have been developed and have a wide range of applicability, but, as we show in this article, they lack accuracy for vibration based material properties identification. This article first demonstrates that a very accurate response surface approximation can be constructed by using dimensional analysis. Second, the article investigates how the accuracy of the approximation used propagates to the accuracy of the elastic constants identified from vibration experiments. For a least squares identification approach, the approximate analytical solution led to physically implausible properties, while the high-fidelity response surface approximation obtained reasonable estimates. With a Bayesian identification approach, the lower-fidelity analytical approximation led to reasonable results, but with much lower accuracy than the higher-fidelity approximation. The results also indicate that standard least squares approaches for identifying elastic constants from vibration tests may be ill-conditioned, because they are highly sensitive to the accuracy of the vibration frequencies calculation.

Keywords Identification · Bayesian identification · Response surface approximations · Dimensionality Reduction · Plate vibration

1 Introduction

Plate vibration has been frequently used for identifying the elastic constants of a plate (Mottershead and Friswell 1993), especially composite laminates. The identification is usually done with free-hanging plates in order to avoid difficult-to-model boundary conditions. Bayesian statistical identification approaches (Kaipio and Somersalo 2005) have the advantage of incorporating in the identification procedure different sources of uncertainty. They can also provide confidence intervals and correlation information on the identified properties. However, the Bayesian method can require Monte Carlo simulation which implies large number of vibration calculations for many combinations of the uncertain parameters such as geometry, material parameters, and boundary conditions. Numerical solutions for free plate vibration natural frequencies, such as Rayleigh–Ritz or finite elements, are too slow to be used in such a context. Accordingly there is a need for simple approximate analytical formulas that can be evaluated very quickly.

A simple, closed-form approximate analytical solution for the vibration problem of orthotropic plates with free boundary conditions was proposed by Dickinson (1978). This solution is applicable to wide ranges of geometries and materials, but its accuracy might not be sufficient for identification purpose. The aim of the present paper is twofold.

This is an extended version of paper number 1221 presented at the 8th World Congress on Structural and Multidisciplinary Optimization, Lisbon, Portugal, 1st–5th June 2009.

C. Gogu (✉) · R. Le Riche · J. Molimard
Centre Science des Matériaux et des Structures,
Ecole des Mines de Saint Etienne, 158 cours Fauriel,
42023, Saint Etienne Cedex 2, France
e-mail: christian.gogu@gmail.com

C. Gogu · R. Haftka
Mechanical and Aerospace Engineering Department,
University of Florida, P.O. Box 116250,
Gainesville, FL 32611, USA

Published online: 13 March 2010

First we seek to develop a procedure for a high fidelity, analytical, approximate formula for the natural frequencies of free orthotropic plates based on response surface (RS) methodology. To achieve the desired fidelity the response surface method is combined with dimensional analysis. Our second goal is to assess the effect of the approximation fidelity on the identification results. For this purpose we compare the results of a least squares and a Bayesian identification using the high fidelity RS approximation and the low fidelity closed-form frequency approximations on experimental data obtained by Pedersen and Frederiksen (1992).

In Section 2 we give a quick overview of the approximate analytical solution developed by Dickinson. In Section 3 we apply dimensional analysis to determine the variables of the response surface approximations (RSA) that lead to the best accuracy. In Section 4 we construct the design of experiment for the RSAs and finally, in Section 5, we compare their fidelity to finite element analyses and to that of the analytical solution by Dickinson. In Section 6 we introduce the least squares and Bayesian identification schemes. Section 7 presents the identification results using the high fidelity approximations while Section 8 those with the low fidelity approximation. We provide concluding remarks in Section 9.

2 Dickinson's analytical frequency approximation

The only simple approximate analytical formula for free vibration of orthotropic plates the authors could find was by Dickinson (1978). He applied characteristic beam functions in Rayleigh's method to obtain an approximate formula for the flexural vibration of specially orthotropic plates. The formula for free boundary conditions on all four edges is restated below for convenience.

$$f_{mn} = \frac{\pi}{2\sqrt{\rho h}} \sqrt{D_{11} \left(\frac{G_m}{a}\right)^4 + 2H_m H_n D_{12} \left(\frac{1}{a}\right)^2 \left(\frac{1}{b}\right)^2 + 4J_m J_n D_{66} \left(\frac{1}{a}\right)^2 \left(\frac{1}{b}\right)^2 + D_{22} \left(\frac{G_n}{b}\right)^4} \tag{1}$$

where f_{mn} is the natural frequency of the mode with wave numbers m and n; ρ is the density of the plate; a, b, h its length, width respectively thickness and D_{ij} the plate flexural rigidities. The rigidities D_{ij} are a function of the elastic constants of the ply (E_1, E_2, ν_{12}, G_{12},), related by classical lamination theory; for a detailed construction procedure of the D_{ij} refer to Gürdal et al. (1998). Part of the notations used are also represented in Fig. 1, for a generic vibration mode. G_{i}, H_{i}, J_{i} are constants, depending only on the mode numbers m and n, whose expressions are given in Table 1.

Note that in order to compare the results of (1) to experimental or numerical results one has to associate the mode numbers to the experimentally or numerically obtained mode. The mode number m respectively n is defined (Waller 1939, 1949) by the number of nodal lines perpendicular to the edge x respectively y plus one. How to count the number of nodal lines can however be tricky, especially for low modes that can have circular symmetry, so for a detailed study of the modes and associated mode numbers of free plates we refer to Waller (1939, 1949).

This simple analytical expression is computationally inexpensive, thus a priori suitable for use in statistical methods which require its repeated use a large number of times. However the fidelity of the approximation must also be acceptable for such a use. This analytical approximation was reported to be within 5% of the exact numerical solution (Blevins 1979). It is not clear whether this accuracy is sufficient when used for identifying accurate elastic constants from vibration experiments. Therefore, in the next sections we will also develop more accurate response surface approximations of the natural frequencies.

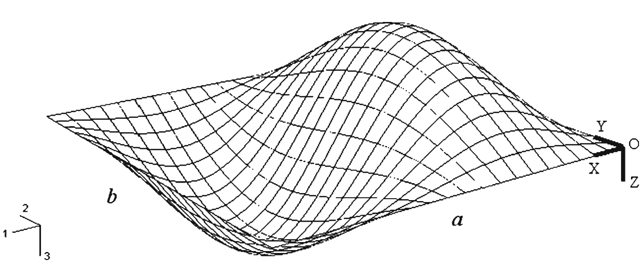

Fig. 1 Plate dimensions and notations. The generic mode represented has mode numbers $m = 2$, $n = 1$

3 Determining nondimensional variables for the RSA

Response surface methodology, also called surrogate modeling, is a technique used to approximate the response of a process which is known only in a finite and usually small number of points. The points where the response is known, which constitute the design of experiments (DoE), are fitted with a particular function depending on the RSA type used. A popular RSA type is the polynomial response surface

Table 1 Expression of the coefficients in the approximate formula for natural frequencies

Mode index i	G_i	H_i	J_i
1	0	0	0
2	0	0	1.216
3	1.506	1.248	5.017
$i\,(i>3)$	$i-\frac{3}{2}$	$\left(i-\frac{3}{2}\right)^2\left(1-\frac{2}{(i-3/2)\,\pi}\right)$	$\left(i-\frac{3}{2}\right)^2\left(1+\frac{6}{(i-3/2)\,\pi}\right)$

(PRS), which uses least-square fit to obtain a polynomial approximation. For more details on RSA techniques refer to Myers and Montgomery (2002).

For elastic constant identification, we propose to fit to finite element simulations of the natural frequencies of the plate a PRS in terms of parameters that may have some uncertainty in their values: ρ, a, b, h and the four D_{ij}, that involve the elastic constants that we seek to identify. We could directly construct a polynomial response surface as a function of these individual model parameters. However, the accuracy of the RSA is generally improved and the number of required simulations is reduced if the number of variables is reduced by using the nondimensional parameters characterizing the problem (Gogu et al. 2009a). To find these parameters we nondimensionalize the equations describing the vibration of a symmetric, specially orthotropic laminate.

Governing equation: $$D_{11}\frac{\partial^4 w}{\partial x^4}+2\left(D_{12}+2D_{66}\right)\frac{\partial^4 w}{\partial x^2\partial y^2}+D_{22}\frac{\partial^4 w}{\partial y^4}+\rho h\frac{\partial^2 w}{\partial t^2}=0$$

where w is the out of plane displacement.

Denoting by M and Q the moment resultants and shear resultants respectively, the boundary conditions are:

On edge $x=0$ and $x=a$ (denoted $x=0;a$):

$$M_x=0\quad\Leftrightarrow\quad -D_{11}\left.\frac{\partial^2 w}{\partial x^2}\right|_{x=0;a}-D_{12}\left.\frac{\partial^2 w}{\partial y^2}\right|_{x=0;a}=0$$

$$Q_x+\frac{\partial M_{xy}}{\partial y}=0\quad\Leftrightarrow\quad -D_{11}\left.\frac{\partial^3 w}{\partial x^3}\right|_{x=0;a}-\left(D_{12}+4D_{66}\right)\left.\frac{\partial^3 w}{\partial x\partial y^2}\right|_{x=0;a}=0$$

On edge $y=0$ and $y=b$ (denoted $y=0;b$):

$$M_y=0\quad\Leftrightarrow\quad -D_{12}\left.\frac{\partial^2 w}{\partial x^2}\right|_{y=0;b}-D_{22}\left.\frac{\partial^2 w}{\partial y^2}\right|_{y=0;b}=0$$

$$Q_y+\frac{\partial M_{xy}}{\partial x}=0\quad\Leftrightarrow\quad -D_{22}\left.\frac{\partial^3 w}{\partial y^3}\right|_{y=0;b}-\left(D_{12}+4D_{66}\right)\left.\frac{\partial^3 w}{\partial x^2\partial y}\right|_{y=0;b}=0$$

This vibration problem involves 11 variables to which we add the variable of the natural frequencies f_{mn} that we seek, so a total of 12 variables for the problem of determining the plate's natural frequency (see Table 2).

These 12 variables involve three dimension groups (m, kg, s). According to the Vaschy–Buckingham theorem (Vaschy 1892; Buckingham 1914) we know that we can have a minimum of $12-3=9$ nondimensional groups.

Posing $\tau=\sqrt{\frac{\rho h a^4}{D_{11}}}$, which is a characteristic time constant, the nine nondimensional groups can be expressed as given in Table 3:

As function of these nondimensional variables the vibration problem can be written as follows:

Governing equation: $$\frac{\partial^4\Omega}{\partial\xi^4}+2\left(\Delta_{12}+2\Delta_{66}\right)\gamma^2\frac{\partial^4\Omega}{\partial\xi^2\partial\eta^2}+\Delta_{22}\gamma^4\frac{\partial^4\Omega}{\partial\eta^4}+\frac{\partial^2\Omega}{\partial\theta^2}=0$$

Boundary conditions:

On edge $\xi=0$ and $\xi=1$ (denoted $\xi=0;1$):

$$-\left.\frac{\partial^2\Omega}{\partial\xi^2}\right|_{\xi=0;1}-\Delta_{12}\gamma^2\left.\frac{\partial^2\Omega}{\partial\eta^2}\right|_{\xi=0;1}=0$$

$$-\left.\frac{\partial^3\Omega}{\partial\xi^3}\right|_{\xi=0;1}-\left(\Delta_{12}+4\Delta_{66}\right)\gamma^2\left.\frac{\partial^3\Omega}{\partial\xi\partial\eta^2}\right|_{\xi=0;1}=0$$

Table 2 Variables involved in the vibration problem and their units

Variable	f_{mn}	w	x	y	a	b	t	ρh	D_{11}	D_{12}	D_{22}	D_{66}
Unit	$\frac{1}{s}$	m	m	m	m	m	s	$\frac{kg}{m^2}$	$\frac{kg\times m^2}{s^2}$	$\frac{kg\times m^2}{s^2}$	$\frac{kg\times m^2}{s^2}$	$\frac{kg\times m^2}{s^2}$

Table 3 Nondimensional parameters characterizing the vibration problem

Nondimensional parameters	$\Omega = \dfrac{w}{h}$	$\theta = \dfrac{t}{\tau}$	$\xi = \dfrac{x}{a}$	$\eta = \dfrac{y}{b}$
$\Psi_{mn} = \tau f_{mn}$	$\Delta_{12} = \dfrac{D_{12}}{D_{11}}$	$\Delta_{22} = \dfrac{D_{22}}{D_{11}}$	$\Delta_{66} = \dfrac{D_{66}}{D_{11}}$	$\gamma = \dfrac{a}{b}$

On edge $\eta = 0$ and $\eta = 1$ (denoted $\eta = 0;1$):

$$-\Delta_{12} \left.\frac{\partial^2\Omega}{\partial\xi^2}\right|_{\eta=0;1} - \Delta_{22}\gamma^2 \left.\frac{\partial^2\Omega}{\partial\eta^2}\right|_{\eta=0;1} = 0$$

$$-\Delta_{22}\gamma^3 \left.\frac{\partial^3\Omega}{\partial\eta^3}\right|_{\eta=0;1} - (\Delta_{12} + 4\Delta_{66})\,\gamma \left.\frac{\partial^3\Omega}{\partial\xi^2\partial\eta}\right|_{\eta=0;1} = 0$$

We seek an RSA only of the nondimensional natural frequency Ψ_{mn}, so we are not interested here in the mode shapes. Accordingly we do not need the nondimensional mode shape Ω, and the nondimensional frequency does not depend on the nondimensional time θ, nor on the nondimensional coordinates ξ and η. This means that the nondimensional natural frequency Ψ_{mn} can be expressed as a function of only four nondimensional parameters $\Psi_{mn} = \Psi_{mn}(\Delta_{12}, \Delta_{22}, \Delta_{66}, \gamma)$.

Note that rewriting the analytical approximation of (1) in its nondimensional form leads to a polynomial function of the nondimensional parameters:

$$(\psi_{mn})^2 = \frac{\pi^2}{4}\Big(G_m^4 + 2H_m H_n \Delta_{12}\gamma^2 + 4J_m J_n \Delta_{66}\gamma^2 + \Delta_{22}\gamma^4 G_n^4\Big) \qquad (2)$$

Equation (2) is a cubic polynomial in Δ_{12}, Δ_{22}, Δ_{66} and γ^2. We will therefore express the squared nondimensional frequency as a cubic polynomial response surface (PRS) in terms of these four variables. Such a PRS has 31 additional polynomial terms beyond those in (2), which can potentially increase the fidelity of the response surface approximation.

4 Constructing the RSA

To fit the RSA we need to sample points in the four-dimensional space of the nondimensional parameters. The ranges of the sampling space depend on the application, and we selected experiments carried out by Pedersen and Frederiksen (1992) for comparing the analytical and RS approximations. If we sampled in the nondimensional variables directly, it would be difficult to deduce values for the dimensional variables needed for the FE model (E_1, E_2, ν_{12}, G_{12}, a, b, h and ρ). Accordingly we chose the following procedure to obtain the points in the nondimensional space and their corresponding dimensional parameters:

1. Sample 5,000 points in the eight dimensional-variables space $\{E_1, E_2, \nu_{12}, G_{12}, a, b, h, \rho\}$ with uniform Latin hypercube sampling within the bounds considered for the problem. The Matlab routines from the Surrogate Toolbox (Viana and Goel 2009) were used for this step.
2. Out of the 5,000 points extract N points in the nondimensional space by maximizing the minimum (max–min) distance between any two points. N is chosen to be either 200 or 250 in the next sections. These steps ensure that the points are well distributed (space-filling) in the nondimensional space.

Figure 2 illustrates this procedure in a two-dimensional case with Δ_{12} and γ only. The blue crosses are representative of the 5,000 points sampled in step 1. The red circles are representative of the 200 points selected in step 2. Because we stop the max–min search after 100,000 iterations (to keep computational cost reasonable) we might not have reached the exact maximum minimum distance, but this is not required for good accuracy of the RSA.

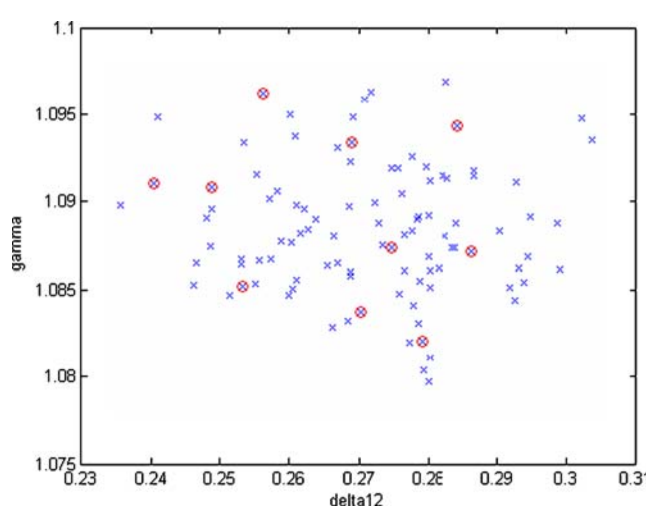

Fig. 2 Illustration of the procedure for sampling points in the nondimensional space

Table 4 Wide bounds (WB) and narrow bound (NB) on the model input parameters

		E_1 (GPa)	E_2 (GPa)	ν_{12}	G_{12} (GPa)	a (mm)	b (mm)	h (mm)	ρ (kg/m^3)
WB	Low bound	43	15	0.2	7	188	172	2.2	1,800
	High bound	80	28	0.36	13	230	211	3.0	2,450
NB	Low bound	52	18	0.23	8.3	202	185	2.55	2,000
	High bound	70	25	0.32	11	216	200	2.65	2,240

5 Frequency RSA

The RSA is fitted to finite element (FE) simulations of the plate which were performed with the Abaqus® commercial FE software. We used 400 thin plate elements (S8R5) to model the composite plate. A convergence study showed that the discretization error is of the order of 0.05% which is negligible compared to the other sources of uncertainty in the problem (e.g. measurement uncertainty).

In our case, the RSA will be used for the least squares and Bayesian identification of the material properties based on the vibrations experiments from Pedersen and Frederiksen (1992). The plate is a glass-epoxy composite panel with stacking sequence $[0, -40, 40, 90, 40, 0, 90, -40]_s$. We decided to construct two sets of RSAs with two different bounds. This is because we found that we can use somewhat narrower bound for the Bayesian identification RSAs without this compromising the results. This behaviour is most likely due, as will be shown later, to the fact that the least squares identification problem is more ill-conditioned than the Bayesian problem. Table 4 presents the wide bounds (WB) and narrow bounds (NB) used for constructing the two RSA. Note that the bounds on the dimensions and the density are somewhat high, not because we consider very high uncertainty in them but because we wanted the RSA to be usable for plates with slightly different parameters (dimensions, etc) as well.

We constructed a cubic polynomial response surface approximation (PRS) for each of the first ten squared nondimensional natural frequencies as a function of the nondimensional parameters determined in Section 3. We used the procedure described in Section 4, sampling 5,000 points within the bounds of Table 4, out of which we extracted $N = 250$ points that are used for the RSA construction. The resulting response surface approximations are denoted RSA_{WB} respectively RSA_{NB}. Note that moving from the nondimensional frequency RSA predictions to the dimensional frequency is done using the equations of Table 3.

To estimate the accuracy of the RSAs, we tested them with 200 additional finite element simulations at points sampled using the same procedure as described in the previous section, using the bounds given in Table 4. The results are given in Table 5, f_i being the dimensional frequencies in order of increasing frequency values. The reader can also refer to Table 6 to get an idea of the order of magnitude of the different frequencies.

For comparison we also provide in Table 5 the error of the analytical frequency approximation of (1) (denoted AFA) compared at the same 200 test points.

The average error in the analytical approximation over the first ten frequencies was found to be 4.9%. This is consistent with previous studies (Blevins 1979) which reported the error of using the analytical formula to be about 5%. On the other hand the errors in the RSAs are about an order of magnitude lower.

For these narrower bounds the RSA fidelity achieved was the highest, the mean of the error among the 200 test points being smaller than 0.01% for all the frequencies. The maximum error among the 200 test points was found to be only about 0.06% for the 9th frequency.

Table 5 Mean and maximum relative absolute error among 200 test points of the frequency RSA predictions with wide bounds (denoted RSA_{WB}), narrow bounds (denoted RSA_{NB}) and the analytical frequency approximations (denoted AFA)

Abs. error (%)		f_1	f_2	f_3	f_4	f_5	f_6	f_7	f_8	f_9	f_{10}
Mean	AFA	5.98	8.50	3.47	4.28	7.22	4.68	2.77	5.72	5.75	1.22
	RSA_{WB}	0.033	0.548	0.290	0.032	0.038	0.680	0.667	0.583	1.110	0.590
	RSA_{NB}	0.0043	0.0036	0.0028	0.0045	0.0044	0.0033	0.0029	0.0049	0.0062	0.0046
Max	AFA	6.54	16.28	8.06	9.43	23.32	21.11	18.30	10.28	12.05	10.01
	RSA_{WB}	0.175	4.197	1.695	0.140	0.195	5.219	5.610	3.680	7.834	7.498
	RSA_{NB}	0.0212	0.0328	0.0301	0.016	0.0197	0.0155	0.0096	0.0171	0.0613	0.0413

Table 6 Experimental frequencies from Pedersen and Frederiksen (1992)

Frequency	f_1	f_2	f_3	f_4	f_5	f_6	f_7	f_8	f_9	f_{10}
Value (Hz)	172.5	250.2	300.6	437.9	443.6	760.3	766.2	797.4	872.6	963.4
Mode (n,m)	(2,2)	(3,1)	(1,3)	(2,3)	(3,2)	(1,4)	(4,1)	(3,3)	(2,4)	(4,2)

We need to mention at this point that in order to obtain the good quality of the fit for all ten frequency RSAs careful modeling was required. Indeed, initially the RSAs for the frequencies number four to seven were very poor both for the wide and the narrow bounds. Typical values for these frequencies are as in Table 6. We can see that frequencies four and five are relatively close as are six and seven. This is because the corresponding modes are symmetric relatively to the x and y axis and the aspect ratio of the plate is close to one. For each of the N sampling points the dimension parameters vary slightly and for some of these points the two symmetric modes switch, meaning that the x-symmetric mode is lower in frequency than the y-symmetric mode for some points and not for others. This issue of switching modes was resolved by modeling only half of the plate and using symmetry boundary conditions for constructing the RSA for frequencies four to seven. Using X- or Y-symmetry boundary conditions allowed following the same mode for varying plate parameters.

On a final note, while there are other types of surrogate models (e.g. kriging, support vector regression, radial basis neural networks), we limited ourselves here to polynomial response surface approximations. This is because as shown in the previous paragraphs the PRS achieved excellent fidelity.

6 Identification problem

6.1 Identification schemes

We use the low fidelity analytical approximate solution and high fidelity frequency RSAs in two different material properties identification schemes in order to compare the effect of the approximation error on the identified results.

The identification procedure seeks the four orthotropic ply elastic constants (E_1, E_2, ν_{12}, and G_{12}) of a glass/epoxy composite based on the first ten natural frequencies of a $[0, -40, 40, 90, 40, 0, 90, -40]_s$ laminate vibrating under free boundary conditions. We use the values measured by Pedersen and Frederiksen (1992) as experimental frequencies in the identification procedure. For convenience these measured frequencies are also given in Table 6. The plate on which the experiments were done had a length $a = 209$ mm, width $b = 192$ mm, thickness $h = 2.59$ mm and the plate's density ρ was 2,120 kg/m^3.

The first identification scheme is a basic least squares approach. The identified parameters correspond to the minimum of the following objective function:

$$J(E) = \sum_{i=1}^{m} \left(\frac{f_i^{\text{num}}(E) - f_i^{\text{measure}}}{f_i^{\text{measure}}} \right)^2 \tag{3}$$

where $E = \{E_1, E_2, \nu_{12}, G_{12}\}$, f_i^{measure} is the ith experimental frequency from Table 6 and f_i^{num} is a numerical frequency prediction.

The second identification scheme is a Bayesian approach. It seeks the probability distribution function of the material properties given the test results. This distribution can be written as:

$$\pi\left(E/f = f^{\text{measure}}\right) = \frac{1}{K}\pi\left(f = f^{\text{measure}}/E\right) \cdot \pi^{\text{prior}}(E) \tag{4}$$

where π denotes a probability distribution function (pdf), $E = \{E_1, E_2, \nu_{12}, G_{12}\}$ is the four dimensional random variable of the elastic constants, $f = \{f_1 \ldots f_{10}\}$ the ten dimensional random variables of the natural frequencies of the plate and $f^{\text{measure}} = \left\{f_1^{\text{measure}} \ldots f_{10}^{\text{measure}}\right\}$ the instance of the ten measured natural frequencies. π^{prior} is the pdf of E prior to the measurements and $\pi(f = f^{\text{measure}}/E)$ is also called the likelihood function of measuring f^{measure} given E. This function provides an estimate of the likelihood of different values of the elastic constants E given the test results. For additional details on Bayesian method applied to the identification of elastic constants the readers can refer to Gogu et al. (2008, 2009b).

As prior distribution for the properties we assumed an uncorrelated normal distribution characterized by the parameters in Table 7. This is a wide prior distribution corresponding to only vague prior information about the properties. The mean value was chosen on the basis of least

Table 7 Normal uncorrelated prior distribution of the material properties

Parameter	E_1 (GPa)	E_2 (GPa)	ν_{12}	G_{12} (GPa)
Mean value	60	21	0.28	10
Standard deviation	10	5	0.05	1.5

squares identification results carried out in Pedersen and Frederiksen (1992).

The most likely value of the posterior distribution given in (4) is usually taken as the identified property. We have shown in Gogu et al. (2008) that, for a similar vibration problem, the Bayesian identification is generally more accurate than the basic least squares method. The difference between the two approaches depends, however, on the problem and can range from negligible to substantial.

6.2 Sources of uncertainty affecting identification

The Bayesian identification can account for different sources of uncertainty as illustrated in previous studies (Gogu et al. 2008, 2009b). We considered here that three sources of uncertainty are present.

First we assumed normally distributed measurement uncertainty for the natural frequencies. Then we assumed epistemic uncertainty due to modeling error. Since this uncertainty depends on the numerical model considered its implementation will be described in later sections.

Finally we considered uncertainties on the input parameters to the vibration model. Apart from the four material properties, the thin plate model also involves four other parameters: the plate length, width and thickness (a, b and h) and the plate density ρ. These parameters are measured beforehand and are known only with a certain confidence. We assumed these uncertainties to be normally distributed as shown in Table 8.

Note that other sources of uncertainty, such as ply-angle variability, might be present. For simplicity relative to the goal of the article we chose however to limit ourselves to the sources of uncertainty described in this section.

7 Identification using the response surface approximation

As mentioned earlier, the least squares identification will use the RSAs with wide bounds (denoted $\mathrm{RSA_{WB}}$, see Section 5) while the Bayesian identification will use the RSAs with narrow bounds (denoted $\mathrm{RSA_{NB}}$, see Section 5).

7.1 Least squares identification

The least squares (LS) optimization was carried out first without imposing any bounds on the variables and led to the optimum shown in Table 9. Note that Pedersen and Frederiksen (1992) applied a least squares approach coupled directly to a Rayleigh–Ritz numerical code to identify the elastic constants. The properties that they found are denoted as Pedersen and Frederiksen (1992) values in Table 9 and following.

The differences between the frequencies at the optimal points and the experimental frequencies are given in Table 10. They are relatively small and the identified values are also reasonably close to the values by Pedersen and Frederiksen. This means that the accuracy of the $\mathrm{RSA_{WB}}$ is good enough to lead to reasonable results.

7.2 Bayesian identification

Apart from the model input uncertainty, described in Section 6.2 and which is common to all the cases, the Bayesian model using the frequency RSAs also considered the following uncertainty on the natural frequencies, whose magnitude is specific to the approximation. Additive normal uncertainty was assumed to stem from the inaccuracies in the experimental frequency measurement. We considered a zero mean and a standard deviation varying linearly between 0.5% for the lowest frequency and 0.75% for the highest.

Table 8 Assumed normal uncertainties in the plate length, width, thickness and density (a, b, h and ρ)

Parameter	a (mm)	b (mm)	h (mm)	ρ (kg/m^3)
Mean value	209	192	2.59	2,120
Standard deviation	0.25	0.25	0.01	10.6

Table 9 LS identified properties using the frequency $\mathrm{RSA_{WB}}$

Parameter	E_1 (GPa)	E_2 (GPa)	ν_{12}	G_{12} (GPa)
Identified values	60.9	22.7	0.217	9.6
Pedersen and Frederiksen (1992)	61.3	21.4	0.279	9.8

Table 10 Differences between experimental frequencies and numerical frequencies corresponding to identified properties for LS identification using the frequency RSAs objective function, $[J(E) = 1.7807 \times 10^{-4}]$

Frequency	f_1	f_2	f_3	f_4	f_5	f_6	f_7	f_8	f_9	f_{10}
Difference (%)	0.11	−0.60	0.09	0.88	−0.25	0.30	−0.18	0.38	−0.46	−0.30

The error stemming from the inaccuracies in the RS approximation is of the order of 0.01%, allowing us to neglect it compared to the measurement error. This leads to the error model shown in (5).

$$f_m = f_m^{\mathrm{RSA}}\,(1 + u_m) \quad \text{where}$$
$$u_m \sim N\left(0, \left(0.0075\frac{(m-1)}{10-1} - 0.005\frac{(m-10)}{10-1}\right)^2\right) \qquad (5)$$

The posterior probability distribution function (pdf) of the material properties was calculated using (4) and Monte Carlo simulations. This calculation required about 130 million frequency calculations thus motivating the need for fast to evaluate analytical frequency approximations. This calculation is clearly out of reach of brute force approach, where the Bayesian identification would be coupled directly to the finite element simulations. In contrast, least squares based identification would typically require between 100 and 100.000 evaluations, depending on the conditioning of the problem, which does not always justify the need for surrogate modelling.

The most likely point of the posterior pdf is given in Table 11. The values by Pedersen and Frederiksen (1992) are also provided.

The Bayesian identified values are close to the values from reference (Pedersen and Frederiksen 1992) and also relatively close to the values identified with the RSA based least squares approach in Table 9. Note that the literature values from reference (Pedersen and Frederiksen 1992) are not necessarily the true values. The true values are probably close but reference (Pedersen and Frederiksen 1992) did not provide any uncertainty measure (such as confidence intervals for example). The Bayesian method can on the other hand provide an estimated confidence interval based on the posterior pdf. It is not the objective of the present article to do a complete characterization of the identified posterior pdf, so for additional details we refer to our dedicated paper (Gogu et al. 2009b). Previous studies (Gogu et al. 2008) on a similar vibration identification problem have also shown that the Bayesian most likely point is on average closer to the true values than the least squares estimate.

All in all, using the RSAs in the identification schemes leads to reasonable results which are in agreement with the literature values, whether using the least squares or the Bayesian identification method. This is not surprising since the RSAs have good accuracy allowing both methods to unfold properly.

In the next section we investigate the identification results obtained with the low fidelity analytical approximate solution (Dickinson 1978) which has much poorer accuracy. The poorer accuracy could lead to more significant differences between the two identification methods.

8 Identification using analytical approximate solution

8.1 Least squares identification

Using the low fidelity analytical approximate solution the least squares (LS) optimization was carried out first while imposing bounds on the variables. We imposed on E_1, E_2, ν_{12}, and G_{12} the bounds NB given in Table 4, which seem reasonable for the properties that we are seeking. The results of the optimization are given in Table 12. The norm of the residuals (i.e. the value of the objective function) is $J(E) = 0.019812$.

We note that several variables hit the bounds. We could keep these results since the bounds we imposed are quite

Table 11 Most likely point of the posterior pdf using the frequency $\mathrm{RSA}_{\mathrm{NB}}$

Parameter	E_1 (GPa)	E_2 (GPa)	ν_{12}	G_{12} (GPa)
Identified values	61.6	20.3	0.280	10.0
Pedersen and Frederiksen (1992)	61.3	21.4	0.279	9.8

Table 12 LS identified properties using the analytical approximate solution (bounded variables; variables denoted with * have hit a bound)

Parameter	E_1 (GPa)	E_2 (GPa)	ν_{12}	G_{12} (GPa)
Identified values	52.0*	25.0*	0.298	8.3*
Pedersen and Frederiksen (1992)	61.3	21.4	0.279	9.8

Table 13 Absolute relative differences between the analytical formula approximation and finite element simulations with the material properties identified by Pedersen and Frederiksen (1992)

Frequency	f_1	f_2	f_3	f_4	f_5	f_6	f_7	f_8	f_9	f_{10}
Difference (%)	6.55	13.0	7.02	5.82	5.71	1.74	0.83	7.00	8.41	1.39

wide and from a physical point of view based on prior knowledge it is quite unlikely that the true parameters lie outside the bounds. We wanted however to also know what happens when imposing no bounds at all and the corresponding results are provided in the Appendix 1. The identified values are significantly worse since some of the identified parameters have physically impossible values.

The unbounded identification also showed that the problem is relatively ill-conditioned due to a flat objective function around the optimum. This emphasizes the importance of high fidelity frequency approximations in order to avoid low accuracy on the optimum estimate.

The least squares identification with the low fidelity analytical approximation thus leads to significantly worse results than the same identification using the high fidelity response surface approximations. To gain additional insight we checked whether the approximate analytical formula by Dickinson might be particularly inaccurate around the actual properties of the plate. Accordingly we provide in Table 13 the difference between formula's predictions and finite element results, both obtained for the material properties identified by Pedersen and Frederiksen (1992).

The results show that analytical formula has an average error for the ten frequencies of about 5.7%, thus not being significantly more inaccurate than what we had found earlier in Table 5. This means that the poor identification results do not appear to be due to particularly poor accuracy of the formula only around the actual values of the properties. Instead, as will be shown later, the flatness of the least-squares objective function leads to error amplification or ill-conditioning.

8.2 Bayesian identification

On top of the model input uncertainty, described in Section 6.2, the present Bayesian identification considered the following uncertainty on the natural frequencies. As for the high fidelity RSA identification in Section 7.2, the uncertainty was assumed to have two sources. The first is due to the inaccuracy in the analytical approximation. The error in the formula was shown in Section 5 to be typically of the order of 5% so a normally distributed uncertainty with standard deviation of 5% was assumed. A second additive uncertainty was assumed to stem from the inaccuracies in the experimental measurement of the natural frequencies. As in Section 7.2 this uncertainty was assumed normal, with the standard deviation varying linearly between 0.5% for the lowest frequency and 0.75% for the highest.

The likelihood function and the posterior probability distribution function (pdf) of the material properties were calculated using (4). The most likely point of the posterior pdf is given in Table 14. Note that with the Bayesian identification, bounds on the material properties do not apply, since the prior distribution assumes this regularization purpose.

The results of the Bayesian identification obtained with low fidelity analytical approximations are again significantly poorer than the results obtained using the high fidelity response surface approximations in Section 7.2. This illustrates again the importance of having high fidelity frequency approximations in order to obtain accurate identification results on this vibration based problem.

On a side note we observe that in spite of using the approximate analytical frequency solution which led to very poor results with the least squares formulation, using the Bayesian approach we identified properties that are physically plausible, even if they are still very far from the values in Pedersen and Frederiksen (1992). This is partly due to the Bayesian identification accounting for the different sources of uncertainty we described earlier. To have additional understanding of what is happening in the two identification cases we compared graphically the two approaches in Appendix 2. This showed that the least squares problem appears to be significantly more ill-conditioned than the Bayesian problem.

On a final note, it might be tempting to draw conclusions at this point as to the comparison of least and Bayesian identification accuracies. This is however outside the scope of the article which aims only the comparison between low and high fidelity approximations. We refrained

Table 14 Most likely point of the posterior pdf using the analytical approximate solution

Parameter	E_1 (GPa)	E_2 (GPa)	ν_{12}	G_{12} (GPa)
Identified values	47.2	27.6	0.290	9.4
Pedersen and Frederiksen (1992)	61.3	21.4	0.279	9.8

from a comparison between least squares and Bayesian identification because it would be quite tricky since the results with the low and high fidelity approximations point in different directions, thus preventing any clear cut conclusions. For a thorough comparison of least squares and Bayesian identification we refer the reader to Gogu et al. (2008), article which breaks down several effects affecting the two identification approaches.

9 Conclusions

The first part of this article was devoted to approximating the natural frequencies of a vibrating orthotropic plate by polynomial response surface approximations (RSA). While the method and the obtained expressions are relatively simple, it can achieve high fidelity, allowing it to be used in most applications that require fast function evaluations together with high fidelity such as Monte Carlo simulation for Bayesian identification analysis. The RSAs constructed were between one and two orders of magnitudes more accurate than previously existing approximate analytical formulas for vibration of free orthotropic plates. To achieve such high fidelity, the RSAs were fitted to the nondimensional parameters characterising the vibration problem.

Note that the overall procedure is applicable not only to free but any boundary conditions as long as the RSAs are refitted to the corresponding design of experiments in terms of the nondimensional parameters characterizing the vibration problem with the specific boundary conditions.

In the latter part, we showed that the fidelity of the frequency approximation has a significant impact on the material properties identification problem we consider. High fidelity approximations such as the nondimensional frequency RSAs can be used independently with least squares or Bayesian identification schemes and lead to reasonable results.

Frequency approximations with errors of the order of 5% such as the analytical approximate solution by Dickinson may be perfectly adequate for applications such as design or uncertainty propagation. They can however lead to unreasonable identification results. Using a least squares approach led in our case to physically implausible results. The Bayesian approach, while always obtaining physically reasonable results, was still substantially less accurate than the identifications using the high fidelity approximations. While the fact that the high fidelity RSA lead to more accurate results than the low fidelity approximate analytical formula would be expected, the magnitude of the error with the low fidelity approximation is worth drawing attention to: the error was amplified from an average of 5% on the natural frequencies to an average between 15% and 270%, depending on the case, when moving to the identified properties.

Acknowledgments This work was supported in part by the NASA grant NNX08AB40A. Any opinions, findings, and conclusions or recommendations expressed in this material are those of the author(s) and do not necessarily reflect the views of the National Aeronautics and Space Administration.

Appendix 1: Unbounded least squares optimization results for the low fidelity approximation

Considering that the bounded least squares optimization of Section 8.1 hit the bounds we did the optimization again, this time without imposing any bounds. The optimum found is given in Table 15. The residuals between the frequencies at the optimal points and the experimental frequencies are given in Table 16. The norm of the residuals (i.e. the value of the objective function) is $J(E) = 0.019709$.

It is obvious from the identified results that the optimum found is not plausible. Not only are the parameters quite far away from the literature values but the Poisson's ratio and shear modulus have negative values. While a negative Poisson's ratio could in theory be possible, negative shear modulus has no physical meaning.

For comparison we also provide the difference between the experimental frequencies and the numerical frequencies at the identified properties for the bounded LS identification case of Section 8.1. It is worth noting that for the unbounded case, in spite of the implausible optimum, the residuals are not very large. All are of the order of a few percent, which for recall is also the order of the accuracy of the analytical approximate solution compared to finite element analyses (see Table 5). It is also worth noting that the residuals and their norm remain practically unchanged compared to the bounded optimization (Table 17). This is a sign of the ill-conditioning of the least squares problem due to a very flat objective function around the optimum. It hints that the accuracy of the frequency approximation has a large effect on the identified results and while a few percent error might seem very reasonable for some application, it can lead to extremely bad results when applied to the present identification problem.

Table 15 LS identified properties using the analytical approximate solution (unbounded variables)

Parameter	E_1 (GPa)	E_2 (GPa)	ν_{12}	G_{12} (GPa)
Identified values	71.1	46.2	−0.402	−17.1
Pedersen and Frederiksen (1992)	61.3	21.4	0.279	9.8

Table 16 Differences between experimental frequencies and numerical frequencies corresponding to identified properties for LS identification (unbounded case) using the analytical approximate solution [$J(E) = 0.019709$]

Frequency	f_1	f_2	f_3	f_4	f_5	f_6	f_7	f_8	f_9	f_{10}
Difference (%)	−1.24	6.96	−6.77	1.69	−1.38	−3.00	0.79	1.48	6.25	−6.75

Appendix 2: Graphical comparison of the identification approaches with the low fidelity approximation

To have a better understanding of what is happening in the two identification approaches when using the low fidelity approximate analytical solution, we plot the posterior pdf and the least squares (LS) objective function in a representative plane. Note that both functions are four dimensional, thus problematic to represent graphically. To obtain a meaningful representation of these functions we decided to plot them in the two dimensional plane defined by the following three characteristic points of the problem: the LS bounded optimum, the LS unbounded optimum and the most likely point of the posterior pdf (see Tables 12, 13 and 15 respectively for the coordinates of these points). The posterior pdf as well as the likelihood function of the material properties are represented in Fig. 3.

For comparison purposes the least squares objective function is also represented in this same plane in Fig. 4.

Figure 3b shows that the likelihood function seems to be multimodal since the distribution function has a local peak in the bottom half of the image (we cannot affirm this with certainty since we are looking at a two-dimensional plot of a four-dimensional function and furthermore the least squares results seem to indicate that the lower lobe is rather due to ill-conditioning and not multimodality). This local peak is relatively far away from the area of physically reasonable properties around the points *max Bayes* and *LS bounded*. The global most likely point of the likelihood function is however much closer to this area, which is reassuring.

Figure 3a shows the posterior pdf, that is, the distribution obtained by multiplying the likelihood function by the prior distribution. The prior distribution had the effect of killing the local peak and significantly narrowing down the distribution. This is somewhat unexpected because we assumed a relatively wide prior distribution which in a typical identification problem is expected to have little impact on the results. It is due however to the ill-posedness of the problem which manifested itself in the least square results as well.

Note that on Fig. 3a the point denoted *max Bayes* does not perfectly correspond with the center of the distribution. This is due to the fact that for the graphical representation only 1,000 Monte Carlo simulations were used in the Bayesian approach in order to keep a reduced computational cost. The effect is a relatively noisy likelihood function and posterior pdf, which don't affect however the qualitative conclusions drawn.

Figure 4 shows the objective function of the least squares identification plotted in the same three points plane. As calculated from Tables 12 and 15 the two points *LS bounded* and *LS no bounds* have a very close value of the objective function [$J(E) = 0.019812$ and 0.019709 respectively]. *LS no bounds* has however a slightly lower objective function value, thus making it the global minimum among the two. Of course in reality the point is physically implausible, but without bounds, the low fidelity analytical frequency approximation will mislead an optimizer in this non physical region. Note that from the shapes of Figs. 3b and 4 it could be inferred that *LS no bounds* is a local optimum. This is however not the case, since from the same starting point, the optimizer leads first to the point *LS bounded* than moves continuously to the point *LS no bounds*. Since we used a local optimizer it means that *LS bounded* and *LS no bounds* must be part of the same lobe, but it is difficult to visualize since we only represent a two-dimensional plot of a four-dimensional function. An immediate corollary is that the objective function is flat, since the points *LS bounded* and *LS no bounds*, whose parameters are up to 306% apart, have and objective function, which is only 0.5% different. The flatness of the objective leads to the ill-conditioning of the identification problem. We can note that there are

Table 17 Differences between experimental frequencies and numerical frequencies corresponding to identified properties for LS identification (bounded case) using the analytical approximate solution [$J(E) = 0.019812$]

Frequency	f_1	f_2	f_3	f_4	f_5	f_6	f_7	f_8	f_9	f_{10}
Difference (%)	−1.27	7.06	−6.84	1.64	−1.37	−2.91	0.72	1.77	6.19	−6.70

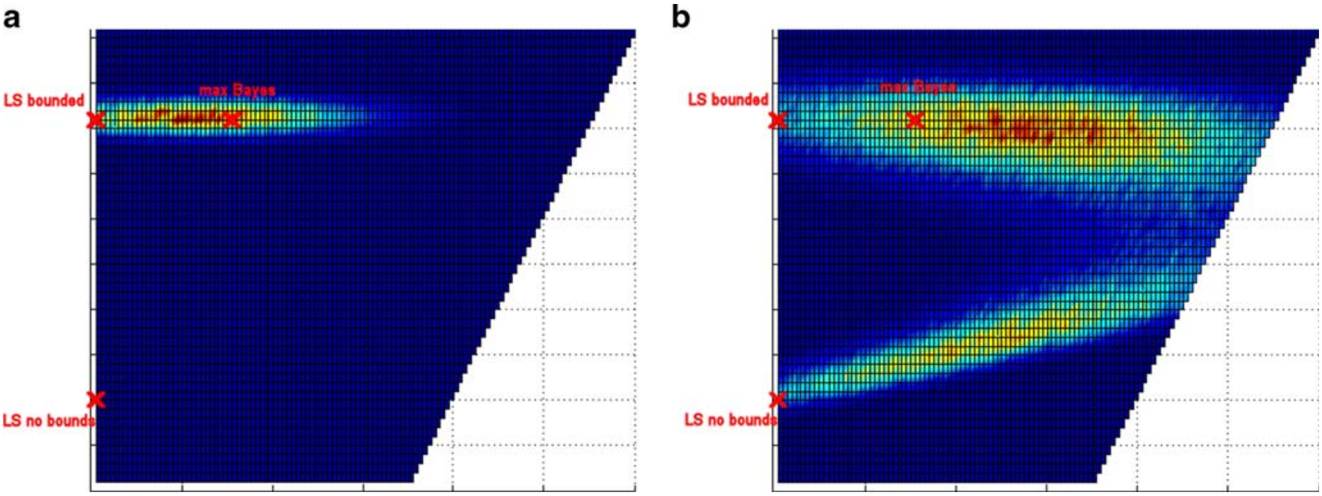

Fig. 3 Two dimensional representation in the three points plane of the posterior pdf (**a**) and the likelihood function (**b**). The three points are: max Bayes = [47.2 GPa, 27.6 GPa, 0.290, 9.4 GPa]; LS bounded = [52.0, 25.0, 0.298, 8.3] and LS no bounds = [71.1, 46.2, −0.402, −17.1]

similarities in shape between the least squares objective function of Fig. 4 and the likelihood function of Fig. 3b. This would be expected since the two are based on the same analytical approximate solution for the frequency calculations, so errors in this approximation would affect the two approaches. However apart from being somewhat shifted, the major difference between the two is that while the LS objective function has the overall minimum in the lower lobe, the likelihood function has the most likely point in the upper lobe, which from a physical point of view is much more plausible. Together with regularization effect of the prior distribution these are some of the reasons why the Bayesian method handles the identification with the low fidelity approximation significantly better than least squares method with this same approximation.

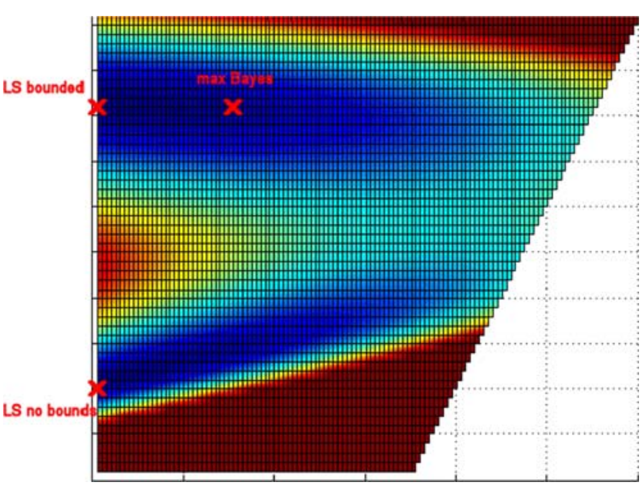

Fig. 4 Two dimensional representation in the three points plane of the least squares objective function

References

Blevins RD (1979) Formulas for natural frequency and mode shape. Van Nostrand Reinhold, New York

Buckingham E (1914) On physically similar systems: illustrations of the use of dimensional equations. Phys Rev 4:345–376

Dickinson SM (1978) The buckling and frequency of flexural vibration of rectangular isotropic and orthotropic plates using Rayleigh's method. J Sound Vib 61:1–8

Gogu C, Haftka RT, Le Riche R, Molimard J, Vautrin A, Sankar BV (2008) Comparison between the basic least squares and the Bayesian approach for elastic constants identification. J Phys: Conf Ser 135:012045

Gogu C, Haftka RT, Bapanapalli S, Sankar BV (2009a) Dimensionality reduction approach for response surface approximations: application to thermal design. AIAA J 47(7):1700–1708

Gogu C, Haftka RT, Le Riche R, Molimard J, Vautrin A, Sankar BV (2009b) Bayesian statistical identification of orthotropic elastic constants accounting for measurement and modeling errors. In: 11th AIAA non-deterministic approaches conference, AIAA paper 2009-2258, Palm Springs, CA

Gürdal Z, Haftka RT, Hajela P (1998) Design and optimization of laminated composite materials. Wiley Interscience, New York

Kaipio J, Somersalo E (2005) Statistical and computational inverse problems. Springer, New York

Mottershead JE, Friswell MI (1993) Model updating in structural dynamics: a survey. J Sound Vib 167:347–375

Myers RH, Montgomery DC (2002) Response surface methodology: process and product optimization using designed experiments, 2nd edn. Wiley, New York

Pedersen P, Frederiksen PS (1992) Identification of orthotropic material moduli by a combined experimental/numerical approach. Measurement 10:113–118

Vaschy A (1892) Sur les lois de similitude en physique. Ann Télégr 19:25–28

Viana FAC, Goel T (2009) Surrogates toolbox v1.1 user's guide. http://fchegury.googlepages.com

Waller MD (1939) Vibrations of free square plates: part I. Normal vibrating modes. Proc Phys Soc 51:831–844

Waller MD (1949) Vibrations of free rectangular plates. Proc Phys Soc B 62(5):277–285